

Magic trapping of a Rydberg ion with a diminished static polarizability

Fabian Pokorný,^{1,*} Chi Zhang,^{1,†} Gerard Higgins,^{1,‡} and Markus Hennrich^{1,§}

¹*Department of Physics, Stockholm University, 10691 Stockholm, Sweden*

Highly excited Rydberg states are usually extremely polarizable and exceedingly sensitive to electric fields. Because of this Rydberg ions confined in electric fields have state-dependent trapping potentials. We engineer a Rydberg state that is insensitive to electric fields by coupling two Rydberg states with static polarizabilities of opposite sign, in this way we achieve state-independent *magic* trapping. We show that the magically-trapped ion can be coherently excited to the Rydberg state without the need for control of the ion's motion.

Introduction.—Atoms and ions in highly-excited Rydberg states are extremely sensitive to external fields, as well as to nearby Rydberg atoms. These strong interactions allow for the creation of atom-photon interfaces [1–3], implementation of nonlinear optics at the few-photon level [4], engineering of atom-atom interactions for quantum computation and simulation [5–7], and for studies of exotic molecular states [8, 9]. Their sensitivity to external electric fields enables the creation of long-lived Rydberg Stark states [10], excellent electric field sensors [11, 12], and near-unity detection of Rydberg states using field ionization. However, fluctuating stray electric fields cause unwanted fluctuating resonance shifts, and in many experiments stray fields must be carefully monitored and corrected. This is particularly difficult when the Rydberg atoms are close to surfaces, as is required for the miniturization of experimental setups [13, 14] and for enhanced microwave (MW) coupling using planar waveguides [15–17].

In this work we reduce the static polarizability of a Rydberg atomic ion, and show that it becomes insensitive to low-frequency electric fields. We accomplish this by coupling two Rydberg states with polarizabilities of opposite sign using a MW field [18, 19]. This allows us to achieve the same trapping potential for an ion in a low-lying electronic (LLE) state and an ion in a Rydberg state, this is called *magic trapping* [20].

When two different electronic states of an atom or molecule experience different trapping potentials there arises coupling between electronic and motional degrees of freedom, as well as motional heating [6]. These effects are usually unwanted and motivate attempts to minimise trapping potential differences, i.e. to achieve magic trapping [21, 22]. In systems of neutral atoms and molecules in optical traps, differences between trapping potentials arise from differences in dynamic polarizabilities [23]; while in our system of charged Rydberg ions in a Paul trap, differences between trapping potentials arise from differences in static polarizabilities [7, 24]. We achieve magic trapping by diminishing a Rydberg state's static polarizability so that it matches the negligible polarizability of a LLE state. We show that with magic trapping coupling between electronic and motional degrees of freedom is mitigated and Rabi oscillations be-

tween a LLE state and a Rydberg state become insensitive to the ion's motional state.

It is worth noting that coupling of Rydberg states using a MW field was previously used to reduce the polarizability difference between two Rydberg states [25, 26]. While this diminishes decoherence on a specific Rydberg transition, reduction of the Rydberg state polarizability to zero stands to be generally applicable in different areas, especially when coherence between Rydberg and LLE states is required.

Theoretical background.—The coupling between two Rydberg states $\{|R_S\rangle, |R_P\rangle\}$ by a MW field is described by the Hamiltonian (with the rotating wave approximation)

$$H = \frac{\hbar}{2} \begin{pmatrix} 0 & \Omega_{\text{MW}} \\ \Omega_{\text{MW}} & -2\Delta_{\text{MW}} \end{pmatrix}, \quad (1)$$

with coupling strength Ω_{MW} and detuning Δ_{MW} . The eigenstates of the coupled system are

$$\begin{aligned} |+\rangle &= \sin\theta |R_S\rangle + \cos\theta |R_P\rangle, \\ |-\rangle &= \cos\theta |R_S\rangle - \sin\theta |R_P\rangle, \end{aligned} \quad (2)$$

where the mixing angle θ is given by

$$\tan(2\theta) = -\frac{\Omega_{\text{MW}}}{\Delta_{\text{MW}}}, \quad (3)$$

and the eigenenergies are

$$E_{\pm} = -\frac{\hbar}{2} \left(\Delta_{\text{MW}} \pm \sqrt{\Omega_{\text{MW}}^2 + \Delta_{\text{MW}}^2} \right). \quad (4)$$

The polarizabilities of the MW dressed states are the weighted averages of the constituent polarizabilities

$$\begin{aligned} \alpha_+ &= \alpha_{R_S} \sin^2\theta + \alpha_{R_P} \cos^2\theta, \\ \alpha_- &= \alpha_{R_S} \cos^2\theta + \alpha_{R_P} \sin^2\theta. \end{aligned} \quad (5)$$

When α_{R_S} and α_{R_P} have opposite signs there exist dressed states $|V_+\rangle$ and $|V_-\rangle$ with vanishing polarizabilities which satisfy

$$\begin{aligned} \alpha_{V_+} &= 0, & \tan^2\theta &= -\frac{\alpha_{R_P}}{\alpha_{R_S}}, \\ \alpha_{V_-} &= 0, & \tan^2\theta &= -\frac{\alpha_{R_S}}{\alpha_{R_P}}. \end{aligned} \quad (6)$$

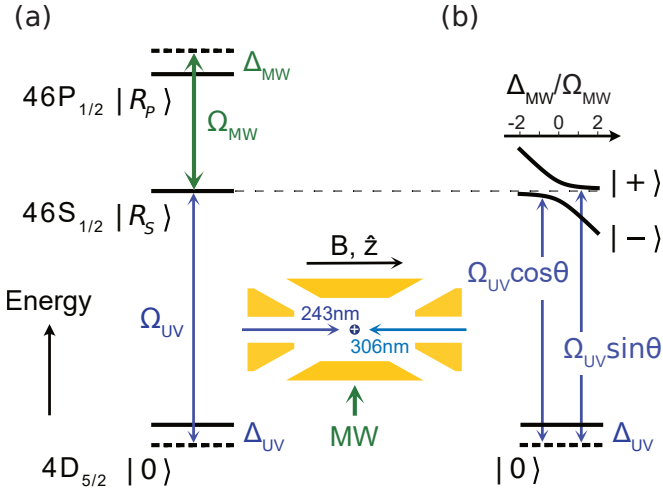


FIG. 1. Level scheme of $^{88}\text{Sr}^+$ showing (a) the bare states and (b) the MW dressed states. Initial state $|0\rangle$ is coupled to Rydberg state $|R_S\rangle$ using a two-UV-photon laser field. A strong 122 GHz MW field couples $|R_S\rangle \leftrightarrow |R_P\rangle$, giving rise to the dressed states $|\pm\rangle$. The inset shows a schematic of the linear Paul trap, the counter-propagating Rydberg-excitation 243 nm and 306 nm laser beams, the MW field, the magnetic field direction and the trap symmetry axis \hat{z} .

Experimental setup.—We work with a single $^{88}\text{Sr}^+$ ion, and couple Rydberg states $|R_S\rangle$ ($46S_{1/2}, m_J = -1/2$) and $|R_P\rangle$ ($46P_{1/2}, m_J = 1/2$) using a MW field near 122 GHz. The ratio of their polarizabilities is $\alpha_{R_P}/\alpha_{R_S} = -4.30$ [27], and we prepare the vanishing-polarizability state $|V_-\rangle = 0.90|R_S\rangle - 0.43|R_P\rangle$ using $\Omega_{\text{MW}}/\Delta_{\text{MW}} = 1.26$.

The ion is confined in a linear Paul trap, and Rydberg states are excited using a two-UV-photon field which couples LLE state $|0\rangle$ ($4D_{5/2}, m_J = -5/2$) to $|R_S\rangle$ with coupling strength Ω_{UV} and detuning Δ_{UV} ($\Omega_{\text{UV}} \ll \Omega_{\text{MW}}$). The relevant level scheme is shown in Fig 1. See [28] for details about the experimental setup and the detection of Rydberg ions. For further details about the MW source we refer to the Supplemental Material [29].

In ion traps the Rydberg energy levels are modulated by the oscillating trapping fields, both by Stark and quadrupole effects [7, 24, 30]. This strongly affects the $|R_S\rangle \leftrightarrow |R_P\rangle$ coupling when $\hbar\Omega_{\text{MW}}$ is not much larger than the amplitude of the energy level modulation. We work in the regime with $\hbar\Omega_{\text{MW}}$ much stronger than the trap effects.

Results.—We probe the MW dressed Rydberg states using spectroscopy as the UV and MW field frequencies are scanned. The results are shown in Fig. 2. The observed resonance lines follow Eq. 4. The asymptotes at $\Delta_{\text{UV}} = 0$ and $\Delta_{\text{UV}} = -\Delta_{\text{MW}}$ correspond to excitation of the bare states $|R_S\rangle$ and $|R_P\rangle$. The resonance lines display an avoided crossing due to the MW coupling. For the data in Fig. 2 the mixing angle θ varies between 0.20 rad and 1.37 rad and the vanishing polarizability states $|V_{\pm}\rangle$ are excited with $\theta = 0.45$ rad and $\theta = 1.12$ rad, respectively.

Next we show that vanishing-polarizability Rydberg states are relatively insensitive to Stark effects. The electric fields used to confine the ion cause Stark shifts, which depend on the ion’s polarizability α . Stark shifts due to trapping fields affect trapped ion precision experiments, including atomic clocks [32, 33], as well as experiments which involve highly-sensitive neutral Rydberg atoms [34], Rydberg molecules [35], and Rydberg ions in ion traps [24, 36, 37]. A Paul trap consists of a combination of static and oscillating electric quadrupole fields. Ideally the nulls of the static and oscillating fields coincide, and at the ion’s equilibrium position the electric field strength is zero. In this case the ion will still be Stark-shifted due to the non-zero electric field it experiences due the spread of its motional wavefunction which extends beyond the trap center. This causes the trapping potential to change and the ion’s trapping frequencies are altered. For a linear Paul trap the altered

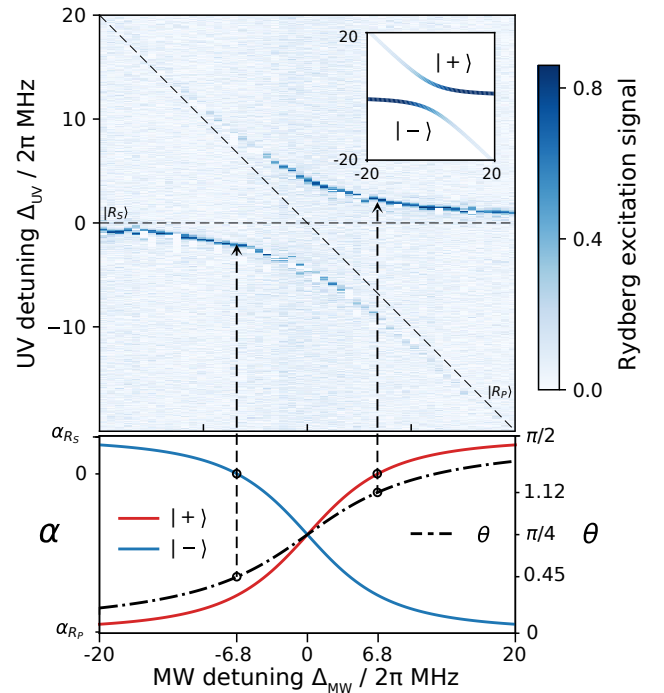


FIG. 2. The character of the dressed states $|\pm\rangle$ can be smoothly varied by tuning Δ_{MW} (or Ω_{MW}). The states are excited by the two-UV-photon field when $\hbar\Delta_{\text{UV}}$ matches the dressed-state energy (Eq. 4). The excitation signal is stronger for states with larger $|R_S\rangle$ admixtures since the two-photon field couples $|0\rangle \leftrightarrow |R_S\rangle$. The bottom part shows the dependence of the dressed state polarizabilities on Δ_{MW} . Vanishing polarizability states $|V_{\pm}\rangle$ with $\alpha_{\pm} = 0$ are highlighted. Here $\Omega_{\text{MW}} = 2\pi \times 8.5$ MHz.

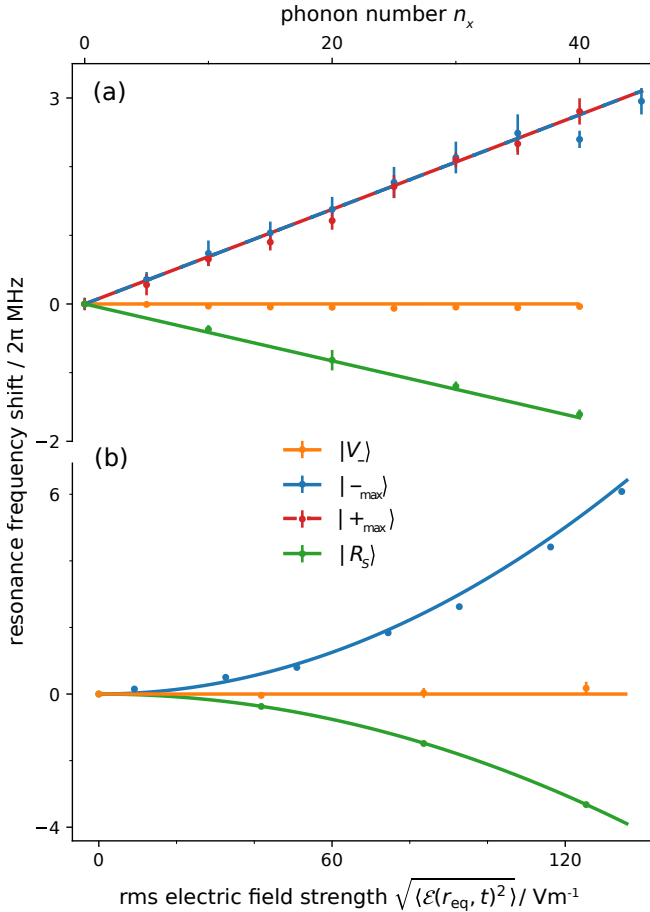


FIG. 3. Rydberg states experience strong Stark shifts. (a) With increasing phonon number the ion experiences stronger electric fields and Stark shifts increase. Maximally-dressed states $|\pm_{\max}\rangle$ show a positive Stark shift while $|R_S\rangle$ shows a negative shift. This confirms that α_{R_P} is larger than and of opposite sign to α_{R_S} . For $|V_-\rangle$, the shift is greatly reduced. The trapping frequencies used are $\{\omega_x, \omega_y, \omega_z\} = 2\pi \times \{1.584, 1.517, 1.020\}$ MHz. (b) Stark shift due to the oscillating electric field at the ion's equilibrium position. $|V_-\rangle$ shows a reduced shift compared to $|R_S\rangle$ and $|-\max\rangle$. We determine $\mathcal{E}(r_{\text{eq}}, t)$ by probing the micromotion sideband of the narrow transition between ground state and $|0\rangle$ [31]. Solid lines are calculated shifts. Error bars represent resonance frequency uncertainties (68% confidence interval), for some data points they are smaller than the marker size.

frequencies are [24]

$$\omega'_{x,y} \approx \sqrt{\omega_{x,y}^2 - \frac{2\alpha A^2}{M}}, \quad \omega'_z \approx \omega_z, \quad (7)$$

where $\omega_{x,y,z}$ are the trapping frequencies in the absence of the Stark effect, x and y are radial directions, z is the axial direction, A is the strength of the oscillating quadrupole field and M is the ion mass. This equation describes usual experimental settings in which the oscillating quadrupole field is much stronger than the static quadrupole field.

As a result the energy required to excite an ion from a LLE state with negligible polarizability to a highly polarizable Rydberg state is Stark shifted depending on the number of phonons in the radial motional modes n_x, n_y

$$\Delta E_{\text{LLE} \rightarrow R} = (n_x + \frac{1}{2}) \hbar (\omega'_x - \omega_x) + (n_y + \frac{1}{2}) \hbar (\omega'_y - \omega_y). \quad (8)$$

The linear relation between the Stark shift and the phonon number can be understood as follows: The root mean square (rms) ion position grows as $\sqrt{n_x}$ ($\sqrt{n_y}$), the rms electric field strength grows linearly with distance from the trap center, and the Stark shift grows with the square of the electric field strength.

We probe this effect by measuring the change of the Rydberg-excitation frequency as n_x is varied (n_y is kept at zero). The results are shown in Fig. 3(a). Rydberg state $|R_S\rangle$ and the maximally-dressed states $|\pm_{\max}\rangle = \frac{1}{\sqrt{2}}(|R_S\rangle \pm |R_P\rangle)$ have large polarizabilities and display large Stark shifts (~ 50 kHz per phonon). We tune the MW coupling to achieve Rydberg state $|V_-\rangle$ which shows greatly-diminished Stark shifts. For $|R_S\rangle$ the altered trapping frequency has a fractional change $(\omega_x - \omega'_x)/\omega_x = 2.6\%$, while $|V_-\rangle$ changes by $(\omega_x - \omega'_x)/\omega_x = (0.145 \pm 0.013)\%$, and thus the trapping potential difference between LLE states and $|V_-\rangle$ is diminished – magic trapping is achieved. We estimate the residual polarizability $\alpha_{V_-} = (0.056 \pm 0.005) \alpha_{R_S}$.

When the nulls of trap's static and the oscillating quadrupole fields do not coincide the ion experiences an oscillating electric field at its equilibrium position $\mathcal{E}(r_{\text{eq}}, t)$, which causes an additional Stark shift [24]

$$\delta = -\frac{1}{2} \alpha \langle \mathcal{E}(r_{\text{eq}}, t)^2 \rangle, \quad (9)$$

where $\langle \rangle$ denotes the time-average over an oscillation period (55 ns in our system). Usually ion trappers aim to overlap the static and the oscillating quadrupole field nulls in order to minimize excess micromotion [31]. We measure the dependence of the Rydberg excitation frequency on the rms electric field strength $\sqrt{\langle \mathcal{E}(r_{\text{eq}}, t)^2 \rangle}$, the results are shown in Fig. 3(b). The resonance frequency shift scales as $\langle \mathcal{E}(r_{\text{eq}}, t)^2 \rangle$, according to Eq. 9. The curvature depends on the Rydberg state's static polarizability α . The vanishing polarizability state $|V_-\rangle$ displays a greatly-diminished response compared to $|R_S\rangle$ and $|-\max\rangle$. The relative curvatures indicate $\alpha_{V_-} = (0.054 \pm 0.016) \alpha_{R_S}$.

The dependence of the Rydberg resonance frequency on the ion's phonon number [Fig. 3(a)] means the electronic and motional degrees of freedom are correlated, and Rydberg resonances are broadened for an ion with a broad thermal phonon distribution [24]. In previous works we mitigated this Stark broadening by using ground state cooling to narrow the phonon number distribution. This allowed us to coherently excite

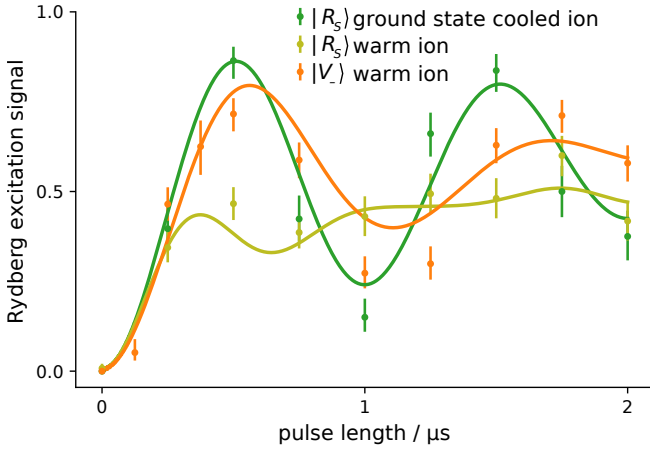


FIG. 4. Rabi oscillations between low-lying electronic state $|0\rangle$ and different Rydberg states. Rabi oscillations are only observed between $|0\rangle$ and $|R_S\rangle$ for a ground-state cooled ion; for a relatively warm (Doppler cooled) ion the oscillations are washed out because of Stark broadening. Rabi oscillations between $|0\rangle$ and $|V_-\rangle$ are driven even when the ion is warm, since $|V_-\rangle$ is insensitive to electric fields. The reduced Rabi-frequency of $|V_-\rangle$ is a consequence of the dressed state’s reduced $|R_S\rangle$ component. Solid lines show simulated results with experimental parameters, using the python module QuTiP [38]. Error bars represent quantum projection noise (68% confidence interval).

highly-polarizable Rydberg states [24, 37] to conduct a Rydberg-entangling gate [39]. In large ion crystals efficient ground-state cooling is impractical and an alternative approach must be followed to avoid the Stark broadening of Rydberg resonances. Here we demonstrate that Rydberg states can be coherently excited without the need for ground state cooling by reducing the Rydberg state polarizability, to achieve magic trapping. Figure 4 shows that Rabi oscillations can be driven between $|0\rangle$ and $|V_-\rangle$ for a relatively warm, Doppler-cooled ion. Rabi oscillations between $|0\rangle$ and $|R_S\rangle$ however are only visible when the ion is ground-state cooled; for a warmer, Doppler-cooled ion with a broad phonon-number distribution the oscillations are smeared out.

Conclusion.—We have used MW dressing to diminish the static polarizability of a Rydberg state, thus diminishing the state’s sensitivity to low-frequency electric fields. In this way we reduce the differences between the trapping potentials of a LLE state and a Rydberg state, to achieve magic trapping. This allows us to coherently excite Rydberg states without careful control of the ion’s motional state. With this method the recent Rydberg ion entangling gate [39] can be carried out in long ion strings [40], in which cooling to the motional ground state is unfeasible.

The reduction of a Rydberg state’s polarizability we demonstrate is directly applicable in a range of Rydberg atom experiments in which care is taken to minimise unwanted Stark effects. For instance, in Rydberg atom

quantum computation and simulation experiments, reducing the sensitivity to electric fields mitigates dephasing errors caused by fluctuating Stark shifts. Of course one must keep in mind that as well as altering the polarizability, MW dressing will affect other Rydberg state properties, such as the lifetime; further it introduces a rotating dipole moment which enables direct dipole-dipole interactions between Rydberg atoms [7, 39].

Acknowledgements.— We thank Weibin Li for theory values of Rydberg state energies and polarizabilities. This work was supported by the Swedish Research Council (Trapped Rydberg Ion Quantum Simulator), by QuantERA project “ERyQSenS”, and by the project “Photonic Quantum Information” (Knut and Alice Wallenberg Foundation, Sweden).

* fabian.pokorny@fysik.su.se

† chi.zhang@fysik.su.se

‡ gerard.higgins@fysik.su.se

§ markus.hennrich@fysik.su.se

- [1] M. Hafezi, Z. Kim, S. L. Rolston, L. A. Orozco, B. L. Lev, and J. M. Taylor, Atomic interface between microwave and optical photons, *Physical Review A* **85**, 020302 (2012).
- [2] J. D. Pritchard, J. A. Isaacs, M. A. Beck, R. McDermott, and M. Saffman, Hybrid atom-photon quantum gate in a superconducting microwave resonator, *Physical Review A* **89**, 010301 (2014).
- [3] L. Sárkány, J. Fortágh, and D. Petrosyan, Long-range quantum gate via Rydberg states of atoms in a thermal microwave cavity, *Physical Review A* **92**, 030303, (2015).
- [4] O. Firstenberg, C. S. Adams, and S. Hofferberth, Non-linear quantum optics mediated by Rydberg interactions, *Journal of Physics B: Atomic, Molecular and Optical Physics* **40**, 152003 (2016).
- [5] M. Saffman, T. G. Walker, and K. Mølmer, Quantum information with Rydberg atoms, *Reviews of Modern Physics* **82**, 2313–2363 (2010).
- [6] M. Saffman, Quantum computing with atomic qubits and Rydberg interactions: Progress and challenges, *Journal of Physics B: Atomic, Molecular and Optical Physics* **49**, 202001 (2016).
- [7] M. Müller, L. Liang, I. Lesanovsky, and P. Zoller, Trapped Rydberg ions: from spin chains to fast quantum gates, *New Journal of Physics* **10**, 093009 (2008).
- [8] J. P. Shaffer, S. T. Rittenhouse, and H. R. Sadeghpour, Ultracold Rydberg molecules, *Nature Communications* **9**, 1965 (2018).
- [9] M. T. Eiles, Trilobites, butterflies, and other exotic specimens of long-range Rydberg molecules, *Journal of Physics B: Atomic, Molecular and Optical Physics* **52**, 113001 (2019).
- [10] T. Cantat-Moltrecht, R. Cortiñas, B. Ravon, P. Méhaignerie, S. Haroche, J. M. Raimond, M. Favier, M. Brune, C. and Sayrin, Long-lived circular Rydberg states of laser-cooled rubidium atoms in a cryostat, *Physical Review Research* **2**, 022032 (2020).
- [11] H. Fan, S. Kumar, J. Sedlacek, H. Kübler, S. Karimkashi,

- J. P. Shaffer, Atom based RF electric field sensing, *Journal of Physics B: Atomic, Molecular and Optical Physics* **48**, 202001 (2015).
- [12] D. H. Meyer, Z. A. Castillo, K. C. Cox, P. D. Kunz, Assessment of Rydberg atoms for wideband electric field sensing, *Journal of Physics B: Atomic, Molecular and Optical Physics* **53**, 034001 (2020).
- [13] A. Tauschinsky, R. M. T. Thijssen, S. Whitlock, H. B. van Linden van den Heuvell, and R. J. C. Spreeuw, Spatially resolved excitation of Rydberg atoms and surface effects on an atom chip, *Physical Review A* **81**, 063411 (2010).
- [14] S. Bernon, H. Hattermann, D. Bothner, M. Knufinke, P. Weiss, F. Jessen, D. Cano, M. Kemmler, R. Kleiner, D. Koelle, and J. Fortágh, Manipulation and coherence of ultra-cold atoms on a superconducting atom chip, *Nature Communications* **4**, 2380 (2013).
- [15] S. D. Hogan, J. A. Agner, F. Merkt, T. Thiele, S. Filipp, and A. Wallraff, Driving Rydberg-Rydberg Transitions from a Coplanar Microwave Waveguide, *Physical Review Letters* **108**, 063004 (2012).
- [16] T. Thiele, S. Filipp, J. A. Agner, H. Schmutz, J. Deiglmayr, M. Stammeier, P. Allmendinger, F. Merkt, and A. Wallraff, Manipulating Rydberg atoms close to surfaces at cryogenic temperatures, *Physical Review A* **90**, 013414, (2014).
- [17] B. T. Gard, K. Jacobs, R. McDermott, and M. Saffman, Microwave-to-optical frequency conversion using a cesium atom coupled to a superconducting resonator, *Physical Review A* **96**, 013833 (2017).
- [18] W. Li, and I. Lesanovsky, Entangling quantum gate in trapped ions via Rydberg blockade, *Applied Physics B* **114**, 37–44 (2014).
- [19] D. W. Booth, J. Isaacs, and M. Saffman, Reducing the sensitivity of Rydberg atoms to dc electric fields using two-frequency ac field dressing, *Physical Review A* **97**, 012515 (2018).
- [20] A. Derevianko, H. Katori, Colloquium: Physics of optical lattice clocks, *Reviews of Modern Physics* **83**, 331–347 (2010).
- [21] S. Zhang, F. Robicheaux, and M. Saffman, Magic-wavelength optical traps for Rydberg atoms, *Physical Review A* **84**, 043408 (2011).
- [22] A. G. Boetes, R. V. Skannrup, J. Naber, S. J. J. M. F. Kokkelmans, and R. J. C. Spreeuw, Trapping of Rydberg atoms in tight magnetic microtraps, *Physical Review A* **97**, 013430 (2018).
- [23] R. Grimm, M. Weidemüller, and Y. B. Ovchinnikov, Optical Dipole Traps for Neutral Atoms, in *Advances In Atomic, Molecular, and Optical Physics vol. 2*, 95–170 (IEEE Comput. Soc. Press 2000).
- [24] G. Higgins, F. Pokorny, C. Zhang, and M. Hennrich, Highly Polarizable Rydberg Ion in a Paul Trap, *Physical Review Letters* **123**, 153602 (2019).
- [25] L. A. Jones, J. D. Carter, J. D. D. Martin, Rydberg atoms with a reduced sensitivity to dc and low-frequency electric fields, *Physical Review A* **87**, 023423 (2013).
- [26] Y. Ni, P. Xu, J. D. D. Martin, Reduction of the dc-electric-field sensitivity of circular Rydberg states using nonresonant dressing fields, *Physical Review A* **92**, 063418 (2015).
- [27] Theory values for Rydberg state energies and polarizabilities were calculated by Weibin Li.
- [28] G. Higgins, W. Li, F. Pokorny, C. Zhang, F. Kress, C. Maier, J. Haag, Q. Bodart, I. Lesanovsky, and M. Hennrich, Single Strontium Rydberg Ion Confined in a Paul Trap, *Physical Review X* **7**, 021038 (2017).
- [29] See Supplemental Material for more details on the microwave setup.
- [30] G. Higgins, C. Zhang, F. Pokorny, H. Parke, E. Jansson, S. Salim, and M. Hennrich, Observation of effects due to an atom’s electric quadrupole polarizability, arXiv:2005.01957 (2020).
- [31] D. J. Berkeland, J. D. Miller, J. C. Bergquist, W. M. Itano, and D. J. Wineland, D. J., Minimization of ion micromotion in a Paul trap, *Journal of Applied Physics* **83**, 5025–5033 (1998).
- [32] T. Rosenband, D. B. Hume, P. O. Schmidt, C. W. Chou, A. Brusch, L. Lorini, W. H. Oskay, R. E. Drullinger, T. M. Fortier, J. E. Stalnaker, S. A. Diddams, W. C. Swann, N. R. Newbury, W. M. Itano, D. J. Wineland, and J. C. Bergquist, Frequency ratio of Al⁺ and Hg⁺ single-ion optical clocks; metrology at the 17th decimal place, *Science* **319**, 1808–1812 (2008).
- [33] C. Tamm, H. Huntemann, B. Lipphardt, V. Gerginov, N. Nemitz, M. Kazda, S. Weyers, and E. Peik, Cs-based optical frequency measurement using cross-linked optical and microwave oscillators, *Physical Review A* **89**, 023820 (2014).
- [34] N. V. Ewald, T. Feldker, H. Hirzler, H. A. Fürst, and R. Gerritsma, Observation of Interactions between Trapped Ions and Ultracold Rydberg Atoms, *Physical Review Letters* **122**, 253401 (2019).
- [35] S. Schmid, A. Härter, and J. Denschlag, Dynamics of a Cold Trapped Ion in a Bose-Einstein Condensate, *Physical Review Letters* **105**, 133202 (2010).
- [36] T. Feldker, P. Bachor, M. Stappel, D. Kolbe, R. Gerritsma, J. Walz, and F. Schmidt-Kaler, F., Rydberg Excitation of a Single Trapped Ion, *Phys. Rev. Lett.* **115**, 173001 (2015).
- [37] G. Higgins, F. Pokorny, C. Zhang, Q. Bodart, and M. Hennrich, Coherent Control of a Single Trapped Rydberg Ion, *Phys. Rev. Lett.* **119**, 220501 (2017).
- [38] J. R. Johansson, P. D. Nation, and F. Nori, QuTiP 2: A Python framework for the dynamics of open quantum systems, *Computer Physics Communications* **184**, 1234–1240 (2013).
- [39] C. Zhang, F. Pokorny, W. Li, G. Higgins, A. Pöschl, I. Lesanovsky, and M. Hennrich, Submicrosecond entangling gate between trapped ions via Rydberg interaction, *Nature* **580**, 345–349 (2020).
- [40] C. Zhang, F. Pokorny, G. Higgins, and M. Hennrich, Fast two-qubit gate in a 12-ion crystal, in preparation.
- [41] V. V. Parshin, S. E. Myasnikova, Metals reflectivity at frequencies 100-360 GHz, 569-570 (2005).
- [42] M. Naftaly, R. Dudley, Terahertz reflectivities of metal-coated mirrors, *Appl. Opt.* **19**, 3201-3204, (2011).

Appendix: Microwave setup

We generate the MW field outside the vacuum chamber through frequency multiplication of a seed signal. The field is coupled to free-space and guided to the ion position through a view-port (see Fig. 5).

The seed signal is provided by an Anritzu MG3690C

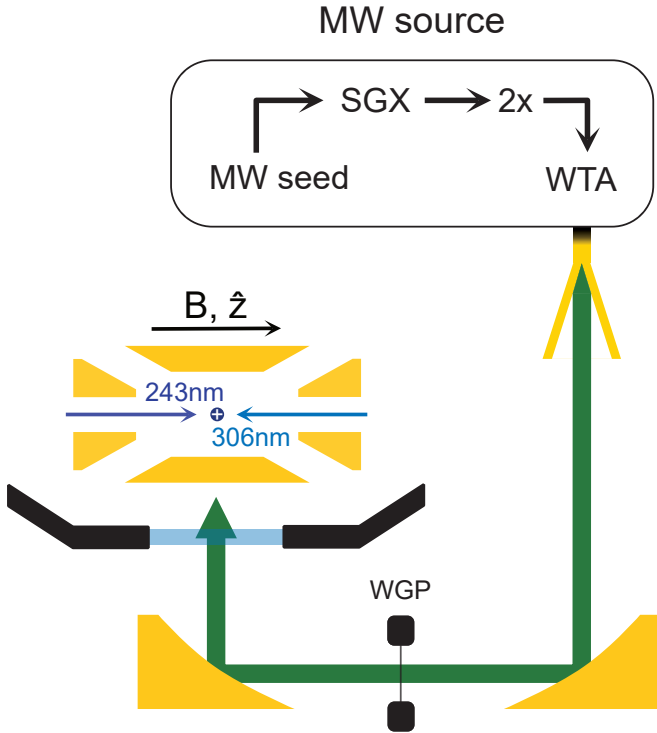


FIG. 5. Schematics of the MW setup and trap. The MW source consists of a MW seed that gets multiplied (first in a SGX unit and then by a doubler) and attenuated before being coupled into free-space with a conical horn antenna. Two off-axis parabolic mirrors guide the field through a view-port into the trap, a wire-grid polarizer (WGP) removes polarization imperfections.

signal generator with an output frequency of 2 – 20 GHz and an output power of 10 dBm. This seed signal feeds a WR15SGX signal generator extension module (SGX) from Virginia Diodes Inc. The SGX multiplies the input signal by a factor of 4 and simultaneously amplifies it; the resulting output signal is 50 – 75 GHz at 20 dBm. An

additional WR8.0X2 frequency doubler (Virginia Diodes Inc) finally results in a field of frequency range of 90 – 140 GHz at 10 dBm output power.

With a WR0.8CH conical horn antenna the MW field is coupled into free space. Two off-the-shelf gold-coated off-axis parabolic mirrors (Thorlabs, Edmund Optics) first collimate and then focus the MW field through a fused silica view-port into the ion trap. The MW field enters the trap perpendicular to the magnetic field and the UV laser beams. Through rotation of the MW source around its axis we can change the polarisation of the field between horizontal and vertical, thus changing between π - and σ - transitions. A $15\ \mu\text{m}$ wire grid polarizer (Pure-Wave Polarizers) placed in the collimated beam removes polarization imperfections.

From the diameter of the conical horn antenna we use geometric optics to estimate the waist of the ≈ 120 GHz MW field to be 10 mm. We measure the transmission of the viewport to be $\approx 70\%$. Manufacturers do not provide data for the reflectivity of gold coatings in the 100 GHz frequency range. However, literature suggests that metal-coated mirrors readily available from standard suppliers perform adequately in the frequency range we are operating [41, 42]; we confirm these findings. We note that the separation between the trap’s blade electrodes is $700\ \mu\text{m}$ and the wavelength for 120 GHz radiation is ≈ 2.5 mm.

We find that the intensity of the MW field inside the trap is high enough to drive the $|46S_{1/2}\rangle \leftrightarrow |46P_{1/2}\rangle$ transition with $\Omega_{\text{MW}} > 2\pi \times 500$ MHz. Such high Rabi-frequencies couple even far off-resonant Rydberg states significantly. In order to diminish such unwanted coupling we attenuate the MW field with a WTA 90-140 waveguide tunable attenuator from Radiometer Physics. This attenuator is placed between doubler and conical horn to prevent underpumping the doubler. The maximum attenuation is 40 dB, resulting in a $\Omega_{\text{MW}} \sim 2\pi \times 8$ MHz.